Temporally Ordered Collective Creep and Dynamic Transition in the Charge-Density-Wave Conductor $NbSe_3$

S. G. Lemay and R. E. Thorne
Laboratory of Atomic and Solid State Physics, Clark Hall, Cornell University, Ithaca, New York 14853-2501

Y. Li and J. D. Brock
School of Applied & Engineering Physics, Cornell University, Ithaca, New York 14853-2501
(Received 22 December 1998)

We have observed an unusual form of creep at low temperatures in the charge-density-wave (CDW) conductor $NbSe_3$. This creep develops when CDW motion becomes limited by thermally activated phase advance past individual impurities, demonstrating the importance of local pinning and related short-length-scale dynamics. Unlike in vortex lattices, elastic collective dynamics on longer length scales results in temporally ordered motion and a finite threshold field. A first-order dynamic phase transition from creep to high-velocity sliding produces "switching" in the velocity-field characteristic.

PACS numbers: 71.45.Lr, 72.15.Nj, 74.60.Ge

Interaction between internal degrees of freedom and disorder determines the dynamical properties of driven periodic media, a class of systems that includes vortex lattices in type-II superconductors [1], Wigner crystals [2], magnetic bubble arrays [3], and charge-density waves (CDWs), the low-temperature phase of quasi-one-dimensional conductors [4]. While the interplay between quenched disorder and elastic deformations is relatively well understood, a complete description of the role of thermal disorder and plastic deformations, which may result in disordered dynamical phases such as driven glass, smectic, and liquid states [5], has not yet been achieved.

CDWs have long been regarded as a prototypical system for the study of many-degree-of-freedom dynamics, both because of their relative theoretical simplicity and because CDW materials such as $NbSe_3$ exhibit collective phenomena with remarkable clarity. A CDW consists of coupled modulations of the electronic density $n = n_0 + n_1 \cos[Q_c x + \phi(x)]$ and of the positions of the lattice ions [4]. Applied electric fields E greater than a threshold field E_T cause the CDW to depin from impurities and slide relative to the host lattice, resulting in a nonlinear dc current density j_c proportional to the CDW's sliding velocity. The impurities cause the CDW to move nonuniformly in both space and time, and the elastic collective dynamics leads to oscillations ("narrow-band noise") in $j_c(t)$. The frequency ν of these oscillations is proportional to the dc component of j_c, and their $Q = \nu/\Delta\nu$ can exceed 30 000 in high-quality $NbSe_3$ crystals.

Despite these simplifying features, most aspects of CDW transport at low temperatures remain poorly understood. At temperatures $T > 2T_P/3$, j_c above E_T is a smooth, asymptotically linear function of E. However, at low temperatures $j_c(E)$ changes drastically, as illustrated in Fig. 1. CDW conduction still begins at E_T but j_c is small and freezes out with decreasing temperature for fields less than a second characteristic field $E_T^* > E_T$. At E_T^*, j_c increases by several orders of magnitude to a more nearly temperature-independent value, often by an abrupt, hysteretic "switch." Similar behavior is observed in all widely studied CDW materials and is thus a fundamental aspect of CDW dynamics [4,6–9].

We have characterized the sliding CDW's transport and structural properties in the low-temperature regime of extremely high-quality $NbSe_3$ crystals. For $E_T < E < E_T^*$, we find that j_c is activated in temperature and increases exponentially with field. Contrary to previous observations in driven periodic media, this creeplike collective motion exhibits temporal order. Our results illuminate the relation between local and collective pinning and indicate that dynamics on lengths much shorter than the Fukuyama-Lee-Rice (FLR) length—neglected in most theoretical treatments—play a central role. They

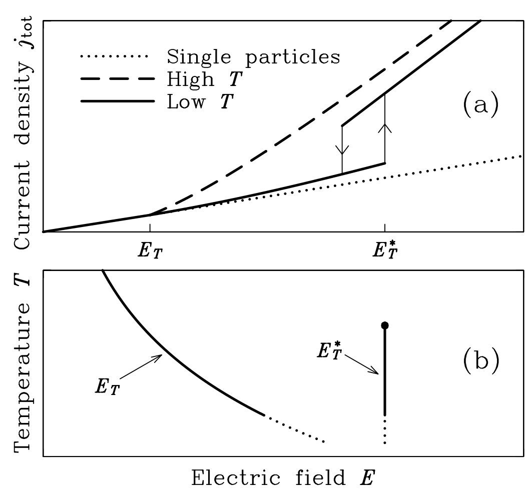

FIG. 1. (a) Form of $j_{tot}(E)$ in the CDW conductor $NbSe_3$. Dotted line: single-particle current density $j_s \propto E$. Dashed line: total current density $j_{tot} = j_s + j_c$ at high temperatures ($T > 2T_P/3$). Solid line: j_{tot} at low T. The difference between the solid or dashed lines and the dotted line gives the CDW current density j_c. (b) Temperature dependence of E_T and E_T^* in $NbSe_3$.

imply revised interpretations for "switching" at E_T^*, the low-frequency dielectric response, low-field relaxation, and nearly every other aspect of the CDW response at low temperatures.

High purity ($r_R \approx 400$) whiskerlike $NbSe_3$ single crystals with typical cross-sectional dimensions of ~ 3 by ~ 0.8 μm were mounted on arrays of 2 μm wide gold-topped chromium wires [10]. The total current density $j_{\rm tot}$ is a sum of the CDW and single-particle current densities, j_c and j_s. j_c is orders of magnitude smaller than j_s in the range $E_T < E < E_T^*$ (except at relatively high temperatures and very close to E_T^* [9]). $j_c(E)$ cannot be directly measured and its form in the low-velocity branch of $NbSe_3$ has not previously been determined. As shown in the inset of Fig. 2, our high-quality crystals [11] exhibit voltage oscillations with Q's as large as 130 in this regime. Consequently, we are able to determine j_c by measuring the oscillation frequency $\nu = (Q_c/2\pi e n_c) j_c$, where $-e$ is the electronic charge, and n_c is the condensed carrier density. $j_c(E)$ was independently estimated by alternating the applied current's direction and measuring resistance transients $R(t)$ associated with transients in the distribution of CDW strain $\epsilon(x) = (1/Q_c)(\partial\phi/\partial x)$ between the current contacts [10,12].

Figure 2 shows the CDW current density $j_c(E) = \nu \times 0.32$ pA$/\mu$m^2 Hz [13] calculated from the measured oscillation frequency $\nu(E)$ for $E_T < E < E_T^*$ at four temperatures. The CDW moves extremely slowly throughout this field and temperature range: the smallest measured ν values at $T = 20.7$ K correspond to CDW motion of roughly one wavelength or 14 Å per sec and to $j_c \approx 10^{-9} j_{\rm tot}$. Between $T \approx 40$ K and $T \approx 20$ K, j_c at fixed $E < E_T^*$ is temperature activated, decreasing by roughly 7 orders of magnitude. j_c jumps abruptly at E_T^*, with $j_c(E = 1.1E_T^*)/j_c(E = 0.9E_T^*)$ increasing from $\sim 10^3$ to $\sim 10^6$ as T decreases from 28 to 20 K.

The current density $j_c \propto \nu$ can be fit by a modified form for thermal creep [14]:

$$j_c(E,T) = \sigma_0(E - E_T)\exp\left(-\frac{T_0}{T}\right)\exp\left(\alpha\frac{E}{T}\right), \quad (1)$$

where the $(E - E_T)$ term describes the fact that the current drops to zero at a threshold E_T that remains large even at high temperatures. The solid lines in Fig. 2 indicate a fit with $T_0 = 505$ K, $\alpha = 136$ K V^{-1} cm, and $\sigma_0 = 350\ \Omega^{-1}\mu$m^{-1}. The value of T_0 is insensitive to the assumed field dependence and corresponds to 0.6 times the single-particle gap 2Δ [15], consistent with measurements of delayed conduction [16] and of σ_c near E_T^* above 30 K [9]. Although creep is observed in other systems, the coherent oscillations imply that the creep in this case is highly unusual: it exhibits temporal order.

Figure 3 shows $j_c(E)$ at $T = 20.5$ K obtained from transient measurements [12]. These data agree closely with $j_c(E)$ deduced from $\nu(E)$ over nearly three decades in j_c [17]. Combining the two measurements yields $j_c/\nu = 0.22$ pA$/\mu$m^2 Hz, consistent with the expected value of $j_c/\nu = 0.32$ pA$/\mu$m^2 Hz [13] within the factor-of-two uncertainty in the value of j_c determined from transient measurements. This rules out significant filamentary conduction, observed in the low-temperature regime of other CDW materials, and implies that the entire crystal cross

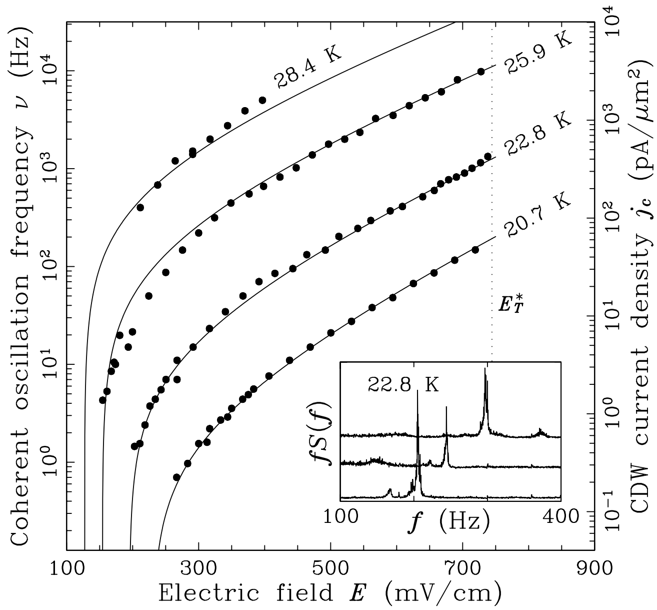

FIG. 2. Coherent oscillation frequency ν and current density j_c versus electric field E. The solid lines are a fit to Eq. (1). The intersection of the lines with the horizontal axis corresponds roughly to the measured E_T at each temperature. The dotted vertical line indicates E_T^*. Inset: Spectral density $S(f)$ at 22.8 K for $E/E_T = 2.63$, 2.77, and 2.88; the curves are offset vertically for clarity.

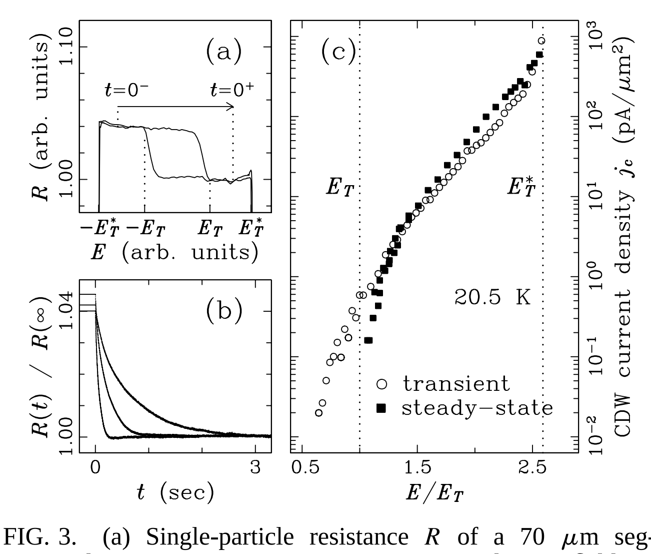

FIG. 3. (a) Single-particle resistance R of a 70 μm segment adjacent to a current contact versus electric field E. (b) $R(t)/R(\infty)$ for the same segment following a reversal of the polarity of E, as indicated by the arrow in (a), for $E/E_T = 1.40$, 1.69, and 1.93. (c) Comparison of j_c calculated from $R(t)$ [12] with j_c obtained from measurements of the coherent oscillation frequency. The current contacts were 630 μm apart, and $E_T(20.5\ \text{K}) = 49$ mV/cm.

section or at least a significant fraction of it is involved in coherent conduction.

Figure 4 shows the results of high-resolution x-ray diffraction measurements of the CDW's transverse structure versus electric field. The CDW creates superlattice peaks in the diffraction pattern, and the half-width of each peak is inversely related to the CDW phase-phase correlation length. For $E < E_T$, the resolution-corrected inverse half-width is $l \approx 4100$ Å, comparable to the crystal dimension in this direction. For $E > E_T$, l decreases monotonically with increasing E, remaining greater than 2500 Å for $E_T < E < E_T^*$. l does not show any abrupt change at E_T^* despite the several orders-of-magnitude increase in j_c there. Similar results were obtained in other directions perpendicular to $\mathbf{Q}_c$ (e.g., [1 0 3] and [1 0 $\bar{2}$]) and at higher temperatures.

Several different models have been proposed to account for the low-temperature properties of CDW conductors. In $K_{0.3}MoO_3$ and TaS_3, whose Fermi surfaces are completely gapped by CDW formation, the activation energies for the single-particle conductivity σ_s and the CDW conductivity σ_c in the low-velocity branch are both comparable to the CDW gap so that $\sigma_c(T) \propto \sigma_s(T)$ [6]. Motivated by this observation, Littlewood [18] suggested that dissipation caused by single-particle screening of CDW deformations limits CDW motion in the low-velocity branch, and that an abrupt, hysteretic transition to the high-velocity branch occurs at a frequency ν comparable to the dielectric relaxation frequency $\nu_1 \propto \sigma_s$ when this screening becomes ineffective. The predicted value of ν at the discontinuity for $K_{0.3}MoO_3$ and TaS_3 is 4 orders of magnitude too large [9], and, for $NbSe_3$ at $T = 20.7$ K, ν is 13 orders of magnitude too large. Levy *et al.* [16] showed that a related model exhibits a hysteretic transition from the pinned state to a fast sliding state when σ_s is small even if high-frequency screening effects are neglected. Neither model can explain the low-temperature CDW properties of partially gapped $NbSe_3$, for which σ_s remains metallic and *increases* with decreasing temperature below 50 K.

Various forms of CDW plasticity, including phase slip at isolated defects [7,8] and shear between two-dimensional

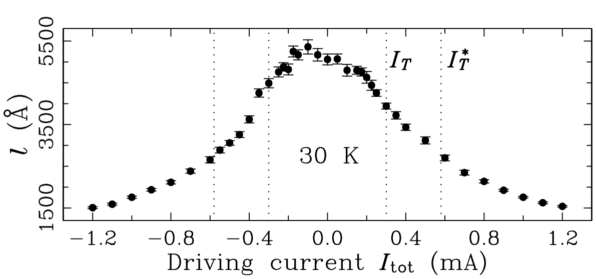

FIG. 4. Inverse CDW peak half-width (corrected for instrumental resolution) in the [1 0 0] direction versus I_{tot}. I_T^* and an upper bound for I_T were determined from measurements of dV/dI_{tot} and of the sharp increase in $1/f$-like noise, respectively.

CDW sheets [19], have been suggested to account for the properties of the low-velocity branch and the transition at E_T^*. Our observation of highly coherent oscillations in high-quality crystals and earlier results [9] rule out models based on slip at rare isolated defects and contacts, and our x-ray measurements rule out the form of shear plasticity discussed in Ref. [19].

Brazovskii and Larkin [20] have focused on the CDW's local interaction with defects. At low temperatures CDW phase advance past rare defects occurs via thermally activated soliton generation, and motion becomes much more rapid at large fields when the effective barrier to soliton generation vanishes. This interpretation has appealing features, but the suggested form for the $j_c(E)$ relation at low temperatures does not reproduce the two branches separated by an abrupt hysteretic transition or the field dependence in either branch observed experimentally in $NbSe_3$. Furthermore, the predicted E_T^* is determined by the soliton energy and should be independent of crystal size. Experimentally, in $NbSe_3$ both E_T and E_T^* vary as $1/t$ for crystal thicknesses t less than ~ 20 μm [9]. The thickness dependence of E_T results because transverse CDW correlations are limited by t so that collective pinning is two dimensional [21]. Consequently, the thickness dependence of E_T^* implies that it, also, is determined by collective effects.

CDW creep of a fundamentally different character is observed in thin $NbSe_3$ crystals at high temperatures [21,22]. Near T_P, E_T is rounded, nonlinear conduction can extend to near $E = 0$, and highly coherent oscillations below the nominal E_T are not observed. This incoherent creep occurs when $k_B T$ approaches the collective pinning energy [$\propto \Delta(T)^2 t$] of the phase-correlated FLR domains, which in $NbSe_3$ have micrometer dimensions. The temporally ordered creep observed in relatively thick crystals at low temperatures above a sharp threshold E_T must involve barriers that are much smaller than those of collective pinning and that are not rare, and a length scale that is much smaller than that of the collective dynamics responsible for the narrow-band noise.

Motivated by earlier ideas [20,23,24], we suggest that the low-velocity branch develops when CDW motion becomes limited by thermally activated phase advance by $\sim 2\pi$ past individual impurities. Although collective pinning is weak [21], the phase of the $Q_c = 2k_F$ oscillations is fixed at each impurity so that phase advance requires CDW amplitude collapse and a finite barrier $\sim\Delta$ [24]. Collective dynamics within volumes containing enormous numbers of impurities (set by the FLR length) then generates the finite threshold E_T and coherent oscillations, as in the high-temperature regime. Unlike in vortex lattices, long-length-scale CDW dynamics is largely elastic and thus retains temporal order even though the short-length-scale dynamics is stochastic.

The $E - E_T$ prefactor [25] and the remaining terms in Eq. (1) follow naturally from this combination of long- and short-length-scale processes. The measured barrier T_0 is consistent with the expected pinning barrier per impurity of $\sim\Delta$ [24]. An applied electric field should reduce this barrier by $\sim en_c V \lambda E$, and, using a condensate density $n_c = 2 \times 10^{21}$ cm^{-3} [4,21], a CDW wavelength $\lambda = 14$ Å, and the measured α value, yields a volume V involved in each thermally activated event of $V \approx 4.2 \times 10^{-17}$ cm^3. Using the scale factor expected for typical impurities [21,26], the bulk residual resistance ratio of $\sim$400 for our crystals corresponds to a concentration $n_i \approx 2.5 \times 10^{16}$ cm^{-3}. The volume per impurity $1/n_i \approx 4 \times 10^{-17}$ cm^3 is thus in excellent agreement with V deduced from creep measurements.

The present experiments together with those of Ref. [9] rule out all previous explanations of the "switching" between low- and high-velocity branches at E_T^* in $NbSe_3$. We suggest that switching occurs via a first-order dynamic phase transition [5,27]. The long-length-scale dynamics exhibits temporal order in both branches, but in the high-velocity branch dynamic fluctuations produced as the CDW moves past impurities may become more important than thermal fluctuations in overcoming impurity barriers [27]. The transition's abruptness, hysteresis, and temperature dependence shown in Fig. 1, the CDW's tendency to fragment near the transition into distinct conducting regions [8], and the field and temperature-dependent time delays required for the transition's completion [16] are all consistent with this explanation.

Finally, we note that local temporal order has very recently been observed in the creep regime of a vortex lattice [28].

We thank C. L. Henley, M. B. Weissman, M. C. Marchetti, A. A. Middleton, and S. Brazovskii for fruitful discussions. This work was supported by NSF Grants No. DMR97-05433 and No. DMR-98-01792. S. G. L. acknowledges additional support from NSERC. The x-ray data were collected using beam line X20A at the National Synchrotron Light Source. Sample holders were prepared at the Cornell Nanofabrication Facility.

[1] G. Blatter *et al.*, Rev. Mod. Phys. **66**, 1125 (1994).
[2] E. Y. Andrei *et al.*, Phys. Rev. Lett. **60**, 2765 (1988).
[3] R. Seshadri and R. M. Westervelt, Phys. Rev. B **46**, 5142 (1992).
[4] See review articles by P. Monceau, G. Gruner, and J. P. Pouget, in *Physics and Chemistry of Low-Dimensional Inorganic Conductors*, edited by C. Schlenker, M. Greenblatt, J. Dumas, and S. van Smaalen, NATO ASI, Ser. B, Vol. 254 (Plenum, New York, 1996).
[5] L. Balents and M. P. A. Fisher, Phys. Rev. Lett. **75**, 4270 (1995); L. Balents, M. C. Marchetti, and L. Radzihovsky, Phys. Rev. B **57**, 7705 (1998), and references therein.
[6] R. M. Fleming *et al.*, Phys. Rev. B **33**, 5450 (1986); G. Mihaly *et al.*, *ibid.* **37**, 1047 (1988); A. Maeda, M. Notomi, and K. Uchinokura, *ibid.* **42**, 3290 (1990).
[7] M. E. Itkis, F. ya Nad', and P. Monceau, J. Phys. Condens. Matter **2**, 8327 (1990); S. V. Zaitsev-Zotov, G. Remenyi, and P. Monceau, Phys. Rev. Lett. **78**, 1098 (1997).
[8] R. P. Hall, M. F. Hundley, and A. Zettl, Phys. Rev. B **38**, 13 002 (1988).
[9] T. L. Adelman *et al.*, Phys. Rev. B **47**, 4033 (1993).
[10] T. L. Adelman *et al.*, Phys. Rev. B **53**, 1833 (1996), and references therein.
[11] These crystals exhibited a single sharp coherent oscillation fundamental at all temperatures and a unique, position-independent switch at low temperatures.
[12] As discussed in Ref. [10], j_c at the midpoint between current contacts just after the current is reversed is given by $j_c(t = 0^+) = (en_c b/\eta)\partial/\partial t[R(t)/\bar{R}]_{t=0^+}$, where b is the length of a short sample segment bounded at one end by a current contact, $R(t)$ is its resistance, $\bar{R}$ is the steady-state value of R, $\eta \approx n_c/n_s \approx 200$, and n_s is the single-particle density.
[13] J. Richard, J. Chen, and S. N. Artemenko, Solid State Commun. **85**, 605 (1993).
[14] P. W. Anderson and Y. B. Kim, Rev. Mod. Phys. **36**, 39 (1964).
[15] A. Fournel *et al.*, Phys. Rev. Lett. **57**, 2199 (1986); T. Ekino and J. Akimtsu, Jpn. J. Appl. Phys. **26**, 625 (1987).
[16] J. Levy and M. S. Sherwin, Phys. Rev. B **48**, 12 223 (1993).
[17] The discrepancy at low E is due to the elastic force associated with the strain profile [10].
[18] P. B. Littlewood, Solid State Commun. **65**, 1347 (1988).
[19] V. M. Vinokur and T. Nattermann, Phys. Rev. Lett. **79**, 3471 (1997).
[20] S. Brazovskii and A. Larkin, Synth. Met. **86**, 2223 (1997).
[21] J. McCarten *et al.*, Phys. Rev. B **46**, 4456 (1992).
[22] J. McCarten *et al.*, Phys. Rev. B **43**, 6800 (1991); J. C. Gill, Synth. Met. **43**, 3917 (1991).
[23] S. Abe, J. Phys. Soc. Jpn. **55**, 1987 (1986); J. R. Tucker, W. G. Lyons, and G. Gammie, Phys. Rev. B **38**, 1148 (1988); I. Baldea, H. Koppel, and L. S. Cederbaum, Phys. Rev. B **52**, 11 845 (1995).
[24] A. Zawadowski and I. Tutto, Synth. Met. **29**, 469 (1989); S. Rouziere, S. Ravy, and J. P. Pouget, Synth. Met. **86**, 2131 (1997).
[25] In $NbSe_3$ in the high-temperature regime, $j_c(E) \propto [E - E_T]^\alpha$ with $\alpha \approx 1$ for $1.2E_T < E < 10E_T$.
[26] This assumes $r_R n_i \approx 1 \times 10^{19}$ cm^{-3}, measured for Ti impurities in Ref. [21], as an estimate for the nonisoelectronic defects that determine r_R in our high-purity crystals.
[27] A. E. Koshelev and V. M. Vinokur, Phys. Rev. Lett. **73**, 3580 (1994).
[28] A. M. Troyanovski, J. Aarts, and P. H. Kes, Nature (London) **399**, 665 (1999).